

# A modified hard-templating for hollow mesoporous silica nanoparticles with suitable particle size and shortened synthesis time

Ngoc Hoi Nguyen<sup>1,2,3</sup>, Cuu Khoa Nguyen<sup>2,3</sup>, Dai Hai Nguyen<sup>1,2,3,\*</sup>

<sup>1</sup>*Institute of Chemical Technology, Vietnam Academy of Science and Technology,  
1A TL29 Street, Thanh Loc Ward, District 12, Ho Chi Minh City, Viet Nam*

<sup>2</sup>*Institute of Applied Materials Science, Vietnam Academy of Science and Technology,  
1B TL29 Street, Thanh Loc Ward, District 12, Ho Chi Minh City, Viet Nam*

<sup>3</sup>*Graduate University of Science and Technology, Vietnam Academy of Science and Technology,  
18 Hoang Quoc Viet, Cau Giay District, Ha Noi, Viet Nam*

\*Emails: [nguyendaihai@iams.vast.vn](mailto:nguyendaihai@iams.vast.vn)

Received: 27 April 2022; Accepted for publication: 24 February 2024

**Abstract.** Hollow mesoporous silica nanoparticles (HMSN), a member of mesoporous silica family synthesized mainly with hard-templating method, has gained great interest in pharmaceutical applications due to their impress characteristics such as good biocompatibility, large specific surface area and pore volume, controllable particle size, large cavity for cargo loading, and flexible surface functionalization possibilities. However, controlling the optimal particle size and shortening the synthesis time have been the issues of HMSN synthesis that needed to be improved. In this study, HMSN was synthesized using hard-templating with some modifications to shorten the synthesis time and adjust the particle size to nearly 100 nm. The obtained HMSN particles showed high uniform morphology as spheres with hollow core-mesoporous shell structure, having the particle diameter of about 90 nm, the hollow diameter of about 68 nm, and the mesoporous shell thickness of about 11 nm. The total time for the main reactions was shortened by more than half from 21 hours to 9 hours. Additionally, MTT assays revealed that the synthesized HMSN was biocompatible material. This modified hard-template method with shorter synthesis time and nearly 100 nm obtained particle diameter would be meaningful for scientific research and industrial scale production.

*Keywords:* hard-templating, hollow mesoporous silica nanoparticle, particle size, HMSN, synthesis time.

*Classification numbers:* 2.3.1, 2.4.3, 2.5.1, 2.10.2.

## 1. INTRODUCTION

Since the first preparation of mesoporous silicate material in the 1990s by Yanagisawa, mesoporous silica nanoparticles (MSN) - the nano form of mesoporous silica, has gained great interest in pharmaceutical applications due to their impressive characteristics such as good

biocompatibility, large specific surface area and pore volume, controllable particle size, and flexible surface functionalization possibilities [1, 2]. Being a member of MSN family, hollow mesoporous silica nanoparticles (HMSN) with a large cavity inside each particle show better drug loading capacity compared to the non-hollow original MSN [3-6]. As the result of this, a lot of studies on the synthesis of HMSN have been conducted with different approaches such as hard-templating, soft-templating and self-templating [6].

Among the HMSN synthesis methods, hard-templating is the most common method due to its advantages such as good synthesis control, predictable and uniform product morphology [7]. With hard-templating, HMSN was synthesized following the three main step procedure including (1) the preparation of the hard template  $dSiO_2$  using Stober method, (2) the preparation of core@shell structure  $dSiO_2@MSN$  using sol-gel technique, and (3) the selective etching of  $dSiO_2@MSN$  to form HMSN [8]. However, besides the well-known advantages of the hard-templating, time consuming is one of its drawbacks that need to be improved. For example, HMSN was prepared with hard-template method in about 21 hours for the main reactions (6 hours for  $dSiO_2$  preparation, 6 hours for  $dSiO_2@MSN$  preparation and 9 hours for  $dSiO_2$  etching) [9, 10]. Therefore, a modified hard-template method shortening the synthesis time would be meaningful for scientists who study on silica nanoparticles as well as for industrial scale production.

Being studied for drug delivery applications, HMSN particle size is one of the most important characteristics that need to be considered in synthesis process. It has been shown that particles with a diameter less than 10 nm tend to be rapidly eliminated by the kidneys, meanwhile particles 200 nm or larger tend to be removed from circulation quicker [11]. There have been several reports about the successful synthesis of spherical HMSN with diameter around 150 to 160 nm [8, 12]. However, 100 nm nanoparticles exhibited the greatest uptake compared to larger diameter particles [13]. Therefore, the optimum size for HMSN should be nearly 100 nm. At this size, HMSN could not only load a sufficient amount of drug, but also prolong the circulation time during the administration.

In this study, HMSN was synthesized using hard-templating with some modifications to shorten the synthesis time and adjust the particle size to nearly 100 nm. Etching through the time of the modified synthesis process was observed and evaluated by scanning electron microscopy (SEM) and transmission electron microscope (TEM). The nanoparticles were characterized by dynamic light scattering (DLS), Zeta potential, Energy dispersive X-ray spectroscopy (EDX), X-ray diffraction (XRD), Fourier-transform infrared (FT-IR) and thermal gravimetric analysis (TGA). In addition, the cytotoxicity of the synthesized HMSN would be evaluated via MTT assays.

## **2. MATERIALS AND METHODS**

### **2.1. Materials**

The chemicals used in the study were reagent grade including tetraethyl orthosilicate (TEOS, 98 %), cetyltrimethylammonium bromide (CTAB, 99 %) ND Sodium carbonate ( $Na_2CO_3$ ) from Sigma-Aldrich (St Louis, MO, USA), ammonia solution ( $NH_3$  (aq), 28 %), triethanolamine (TEA, > 98.0 %) and ethanol (EtOH,  $\geq 99.9$  %) from Scharlau (Spanish).

Dulbecco's Modified Eagle Medium (DMEM), fetal bovine serum (FBS), penicillin and streptomycin were purchased from Sigma-Aldrich (St Louis, MO, USA). The human breast cancer cell line (MCF-7) was obtained from the ATCC (American Type Culture collection,

Manassas, VA). The cells were cultured with complete DMEM (10 % FBS, 100 IU/mL penicillin, and 0.1 mg/mL streptomycin) in a 5 % CO<sub>2</sub> humidified incubator.

## 2.2. Methods

### 2.2.1. Synthesis of hollow mesoporous silica nanoparticles

Hollow mesoporous silica nanoparticles were synthesized through a hard-templating method via three main steps (Figure 1). To control the HMSN particle diameter below 100 nm, the particle size of the hard template dSiO<sub>2</sub> was reduced through the synthesis components such as the concentration of silica precursor TEOS, the concentration of catalyst agent NH<sub>3</sub> and the amount of EtOH [9, 10]. Moreover, the time of mesoporous silica coating step and hard template silica etching step would be shortened through reactional parameters such as temperature and catalyst agent [8].

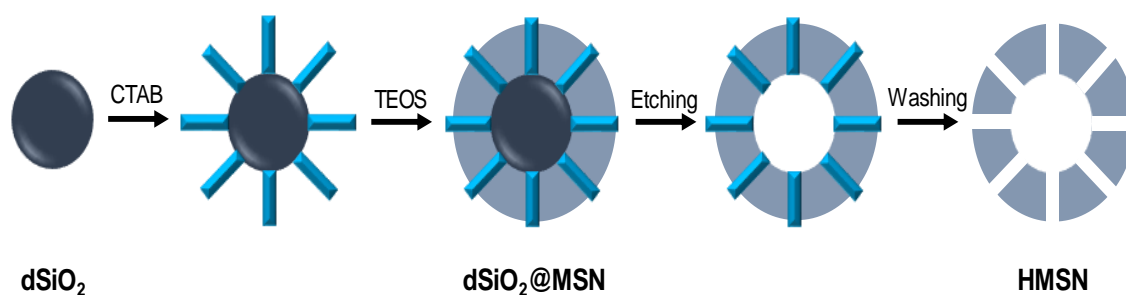


Figure 1. Schematic representation of the synthesis of the hollow mesoporous silica nanoparticles (HMSN) via hard-templating method.

In the first step, dSiO<sub>2</sub> as hard templates were prepared by a modified Stober method from TEOS, NH<sub>3</sub> and EtOH [14]. Typically, 70.0 mL of absolute ethanol was mixed with 10.0 mL deionized water and 3.0 mL of ammonia and stirred for about 15 minutes at 60 °C. Then 6.0 mL of TEOS was added to the mixture and the reaction was allowed to happen for 6 hours. During this step, dSiO<sub>2</sub> particles grew through two consecutive reactions including hydrolysis of TEOS into silanol monomers and subsequently condensation of the silanol monomers into siloxane network [15].

In the second step, mesoporous silica layer was coated on the hard-templates using sol-gel method [8]. A solution including 3.0 g of CTAB, 50.0 mg of TEA and 20.0 mL of deionized water was prepared. Then, 10 mL of the dSiO<sub>2</sub> solution obtained in the first step was added and stirred at room temperature for 1 hour. The mixture was alternately heated to 80 °C, added 0.5 mL of TEOS and stirred for 1 hour to form dSiO<sub>2</sub>@MSN. In this step, CTAB in water would initially form positively charged micelles and electrically bond around the surface of negatively charged hard-template dSiO<sub>2</sub>. The silica precursor TEOS was then added to the reaction media, where hydrolysis of TEOS in alkaline medium (TEA) and condensation of silanol monomers occurred similarly to that in step 1. As a result, a shell was formed with CTAB micelles as the pore generating agent [16].

In the third step, the hard-templates were removed via etching process using an aqueous Na<sub>2</sub>CO<sub>3</sub> solution [5, 17]. The mixture obtained in the second step was cooled down to 50 °C before the addition of Na<sub>2</sub>CO<sub>3</sub> (to reach the concentration of 21.2 mg/mL) and then stirred

continuously to let the etching process happen. In this step, CTAB micelles with inward-facing hydrophobic tails formed channels that allowed the water-soluble alkaline etching agent to pass through and etch the hard-templates. In addition, sufficiently thick walls of these mesopore templates would protect the shell around them. Moreover, the outward-surface of the mesoporous shell would be protected by CTAB micelles [18].

To study the etching of silica hard-template over time, a certain volume of the reaction mixture was aspirated every 30 minutes. The collected samples, named by the etching time including HMSN 30, HMSN 60, ..., HMSN 180, were dialyzed by  $12 \times 14$  kDa membranes against ethanol and distilled water in 3 days before lyophilized.

### 2.2.2. Characterizations of the synthesized hollow mesoporous silica nanoparticles

To evaluate the particle size, morphology and hollow core shell structure of the synthesized samples, the SEM and TEM images were taken on FESEM S-4800 (HITACHI, Tokyo, Japan) and JEM-1400 (JEOL, Tokyo, Japan), respectively. To study the components and evaluate the purity of the synthesized particles, the FT-IR and TGA analyses were carried out. FT-IR investigation was performed on Bruker Equinox 55 FTIR spectrometer (Bruker, Ettlingen, Germany) using KBr pellet method. Additionally, TGA investigation was performed with a TGA Analyzer (Mettler Toledo, Switzerland) under a nitrogen flow with temperature program from 30 to 800 °C at the increasing speed of 10 °C/minute.

BET Surface Area Analysis and BJH Pore Size and Volume Analysis was operated on TriStar II Plus (Version 3.03, Micromeritics, GA, USA) to determine the surface area and mesopore diameter of the particles.

The particle size distribution was determined by the DLS technique, meanwhile the zeta potential ( $\zeta$ ) was determined through a Helium-neon (He-Ne) laser beam with the setting detection angle of 90°, temperature of 25 °C and wavelength of 532 nm using a Zetasizer Nano SZ (SZ-100, Horiba, Kyoto, Japan). X-ray diffraction experiment was performed on a Bruker D2 Phaser diffractometer (Germany) using mono-chromated  $\text{CuK}\alpha$  radiation to investigate the molecular structure of HMSN. Moreover, the EDX analytical method was used for chemical characterization of HMSN.

### 2.2.3. Cytotoxicity study of the synthesized hollow mesoporous silica nanoparticles

Cytotoxicity of the synthesized HMSN was evaluated through the MTT assay on MCF-7 cell line, which was cultivated in complete DMEM (10 % FBS, 100 IU/mL penicillin, and 0.1 mg/mL streptomycin) in a 5 %  $\text{CO}_2$  humidified incubator. The cells were seeded into a 96-well culture plate with a density of  $3 \times 10^4$  cells/well. After 24 h being incubated with the culture media, the cells were treated with the synthesized HMSN at different concentrations from 10  $\mu\text{g/mL}$  to 250  $\mu\text{g/mL}$  for 48 h, then 20  $\mu\text{L}$  of 5 mg/mL MTT solution were added to each well and incubated for 4 h more at 37 °C. The culture medium was discarded, DMSO was added with the amount of 100  $\mu\text{L}$ /well and subsequently shaken for 2 min. Then the absorbance was measured in a microplate reader at the wavelength of 570 nm. The cell viability was calculated using the following equation:

$$\text{Cell viability (\%)} = \frac{\text{Abs}_{\text{sample}} - \text{Abs}_{\text{blank}}}{\text{Abs}_{\text{control}} - \text{Abs}_{\text{blank}}} \times 100 \% \quad (1)$$

### 3. RESULTS AND DISCUSSION

#### 3.1. Synthesis of silica hard-templete

The dSiO<sub>2</sub> particles were obtained after the first step of the HMSN synthesis process. Characteristics of the obtained dSiO<sub>2</sub> including zeta potential, hydrodynamic size and morphology were showed in Figure 2. The synthesized hard-templates had a zeta potential of  $-45.8 \pm 0.41$  mV, which was consistent with the previous reports of silica nanoparticles [19]. The hydrodynamic size of dSiO<sub>2</sub> was determined as  $96.8 \pm 0.26$  nm with polydispersity index (PI) of 0.072. Low PI value ( $< 0.1$ ) indicated that the obtained dSiO<sub>2</sub> was highly uniform with respect to the particle size [20]. As can be seen from SEM and TEM images, the dSiO<sub>2</sub> particles are mono-disperse spheres with particle diameter of  $65.27 \pm 0.42$  nm. Compared to the previous studies, the hard template dSiO<sub>2</sub> diameter reduced from more than 100 nm to about 65 nm [8, 10]. The reduction of the hard template diameter is expected to lead to the reduction of the synthesized HMSN.

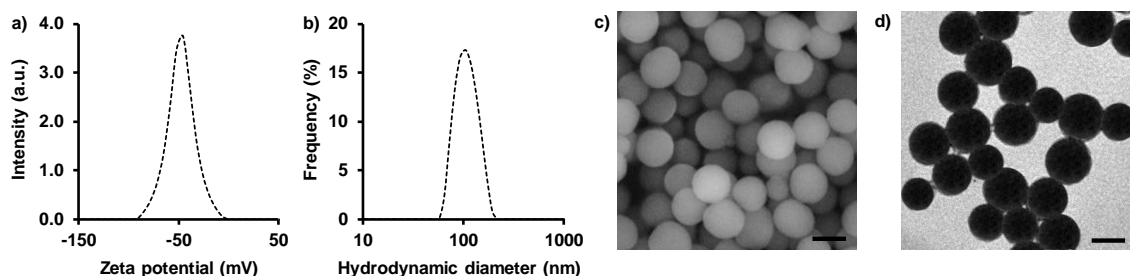


Figure 2. Characterizations of the synthesized hard-template dSiO<sub>2</sub>: a) Zeta potential; b) DLS particle size distribution; c) SEM image; d) TEM image. Scale bar = 50 nm.

#### 3.2. Etching over time of silica hard-templete in the synthesis of hollow mesoporous silica nanoparticles

HMSN particles which was under different etching time from 30 to 180 minutes were taken for SEM and TEM images (Figure 3). SEM images presented the outside appearance of HMSN, showing that the particles had non-hollow core structure after 30 and 60 minutes of etching. The hollow core structure of HMSN was visible after 90 minutes and most obvious after 120 minutes of etching. However, after 150 minutes of etching, the shell appeared to have some holes in it, indicating that it had begun to be corroded but the particles were still spherical. Finally, after 180 minutes of etching, the particles lost their spherical shape and the shell was collapsed.

TEM images showed the status of the hard core which could help explain how the etching process occurred. When the etching agent accessed the core, the rattle-type spheres with double-shell structure would be first obtained (HMSN 30, HMSN 60). After that, the cavity extended toward both sides and consequently the hollow structure was formed (HMSN 90, HMSN 120). When the hard core was totally corroded, the mesoporous shell would be corroded and destroyed by the etching agent (HMSN 150, HMSN 180). This observed phenomenon was consistent with the mechanism of selective etching in the previous report [18]. As previously mentioned, CTAB at sufficient concentration (21.2 mg/mL) would act as a protector for the mesoporous shell and uniform HMSNs with clear hollow cavity would be obtained when the etching process was done (in this case the suitable etching time was determined as 120 min). However, too long etching

time (150 and 180 min) would cause over-etching, leading to the etching of the shells and resulting aggregated particles with rough surfaces. Gradually, the shell became thinner, was destroyed and the particle structure collapsed as seen in Figure 3. These results suggested that the suitable etching time was 120 minutes, consequently the HMSN 120 would be used for further experiment. Importantly, the synthesis time of HMSN for the main reactions in the current study decreased from 21 hours to 9 hours. In details, hard-template preparation time was remained for 6 hours, mesoporous shell coating time shortened to 1 hour and hard-template etching time shortened to 2 hours [10]. This modified hard-template method with shorter synthesis time would be meaningful for scientists who study on silica nanoparticles as well as for industrial scale production.

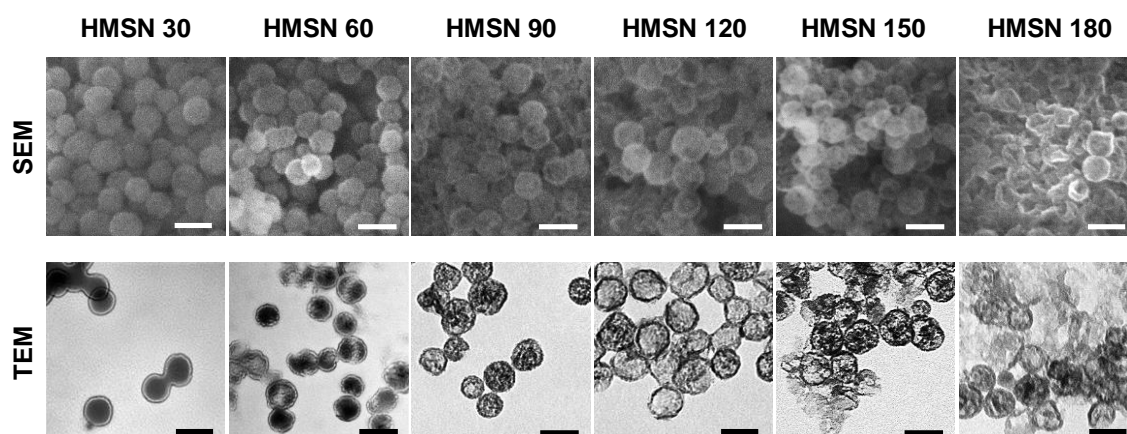


Figure 3. SEM and TEM images of HMSN over etching time. Scale bar = 100 nm.

### 3.3. Characteristics of synthesized hollow mesoporous silica nanoparticles

The synthesized HMSN particles were characterized via TEM, BET, BJH, FT-IR, EDX, Zeta potential, DLS, XRD and TGA analysis whose results were showed in Figure 4 and Figure 5.

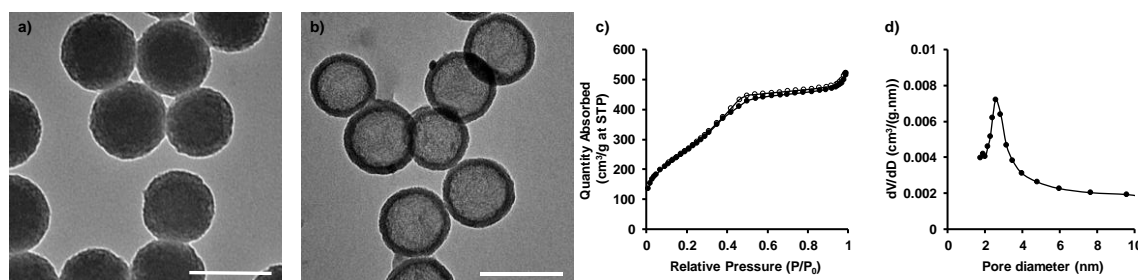
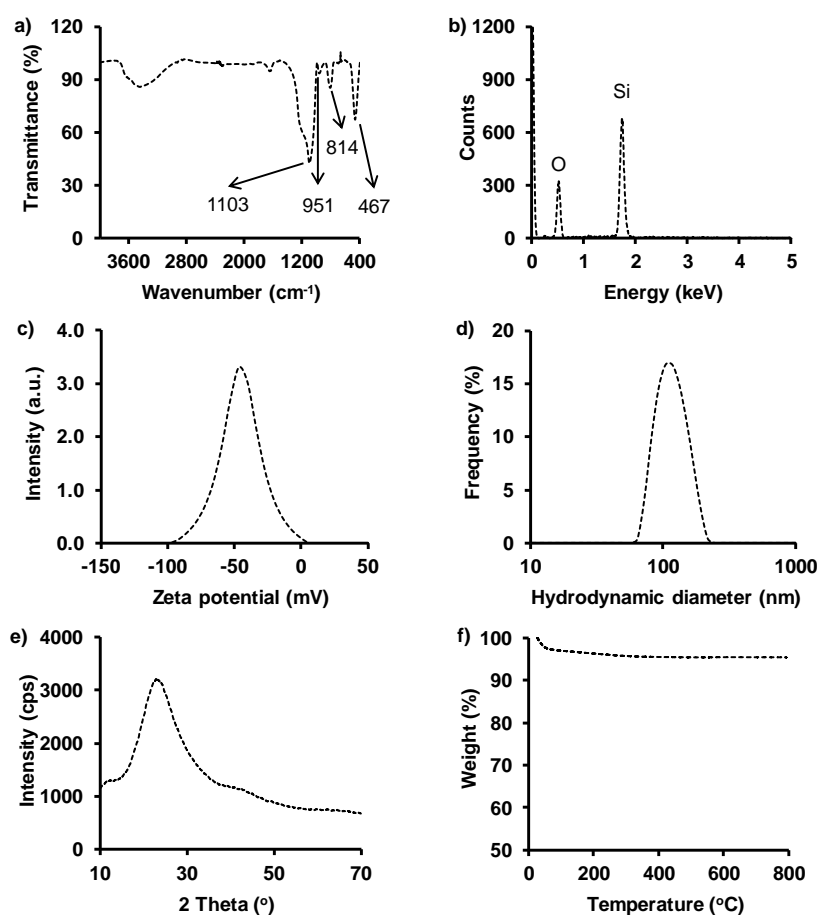


Figure 4. a) TEM image of  $d\text{SiO}_2@\text{MSN}$ ; b) TEM image, c)  $\text{N}_2$  adsorption-desorption isotherms and d) Pore size distributions of the synthesized HMSN. Scale bar = 100 nm.

Based on TEM image in Figure 4a,  $d\text{SiO}_2@\text{MSN}$  particles showed core@shell structure: the inner dark region is the solid core and the surrounding brighter region is the mesoporous shell. Meanwhile, HMSN's TEM image (Figure 4b) clearly showed the hollow@shell structure of the chosen HMSN 120 particles with the particle diameter of  $90.15 \pm 1.29$  nm, the hollow diameter of  $68.73 \pm 0.95$  nm, and the mesoporous shell thickness of about 11 nm. Compared to

the previous studies, the particle size of the synthesized HMSN reduced from over 134 nm to about 90 nm [8, 10]. Recently, nanomaterials have been surface modified with different polymers and functional groups to increase their biocompatibility, drug loading capacity and targeting ability, the particle diameter consequently will increase after being denatured [11]. Therefore, this obtained HMSN would be an appropriate material for a complete nano-carrier preparation. The N<sub>2</sub> adsorption–desorption isotherms and the pore size distributions of HMSN were shown in Figure 4c and Figure 4d. The HMSN's isotherms were classified as Langmuir type IV isotherm curve and type H2 hysteresis loop according to IUPAC, proving mesoporous nature of the synthesized HMSN [21, 22]. Additionally, the surface area and the pore diameter of HMSN were determined as about 767 m<sup>2</sup>/g and 2.5 nm, respectively. These results are in relative agreement with the previous publications [23, 24].



*Figure 5.* Characterizations of the synthesized HMSN: a) FT-IR spectrum; b) EDX spectrum; c) Zeta potential; d) DLS particle size distribution; e) XRD pattern; f) TGA pattern.

As seen from the FT-IR spectrum (Figure 5a), the strong absorption bands at 1103 cm<sup>-1</sup>, 814 cm<sup>-1</sup> and 467 cm<sup>-1</sup> were attributed to the anti-symmetric stretching vibration, symmetric stretching vibration and bending vibration of Si-O-Si, respectively. The characteristic absorption peaks at 3500 cm<sup>-1</sup> and 951 cm<sup>-1</sup> corresponded to the bending vibration of Si-OH [25]. The elemental composition on the surface of HMSN was identified via EDX analysis (Figure 5b). The EDX spectrum showed the presence of oxygen and silicon elements with the atomic

percentages of 68.82 and 31.18, respectively, proving that CTAB and other reacted reagents were well removed [26]. The synthesized HMSN had a zeta potential of  $-46.6 \pm 0.73$  mV (Figure 5c), which was other than  $-30$  mV to  $+30$  mV, would help prevent agglomeration and kept the particles dispersed well [27]. The DLS analysis determined hydrodynamic size of HMSN was  $108.17 \pm 1.83$  nm and PI was 0.083 (Figure 5d). Low PI value ( $< 0.3$ ) indicated that the obtained HMSN was highly uniform with respect to the particle size [20]. Figure 5e showed the XRD patterns of HMSN with un-sharp peak at  $2\theta = 23.93^\circ$ , confirming the amorphous nature of silica particles [28]. Figure 5f presented the TGA curve HMSN. The initial weight loss at temperature below  $200^\circ\text{C}$ , which was about 11.5 %, could be attributed to the physically adsorbed water. In the range of  $200 - 600^\circ\text{C}$ , the weight loss was about 7.0 %. This might due to a small amount of CTAB remaining in the HMSN.

### 3.4. Cytotoxicity of synthesized hollow mesoporous silica nanoparticles

MTT assays on MCF-7 cell line were carried out to evaluate the cytotoxicity of the synthesized HMSN and the results were shown in Figure 6. As can be seen from the Figure 6, the cell viability was 100 % when being treated with  $10\ \mu\text{g/mL}$  HMSN. When the treated concentration of HMSN increased to  $250\ \mu\text{g/mL}$ , the cell viability gradually decreased but remained higher than 80 %. This meant the synthesized HMSN had no obvious toxicity on MCF-7 cells in a range of concentrations from 10 to  $250\ \mu\text{g/mL}$ , demonstrating that the synthesized HMSN in the current study could be regarded as a biocompatible nanocarrier.

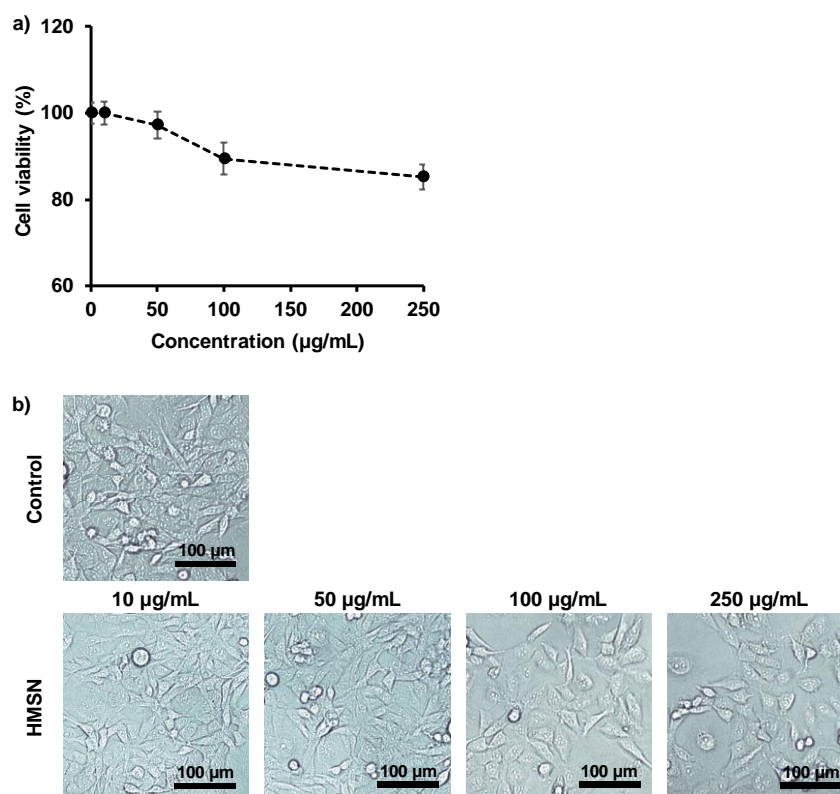


Figure 6. a) Cell viability assay by MTT assay with variable concentrations of HMSN on MCF-7 cells; b) MCF-7 cells treated by HMSN at different concentrations. Scale bar is 100  $\mu\text{m}$ .

#### 4. CONCLUSIONS

The HMSN particles with an optimal diameter were successfully prepared by the modified hard-templating in a shortened synthesis time. The obtained HMSN particles showed high uniform morphology as spheres with hollow core-mesoporous shell structure, having the particle diameter of about 90 nm, the hollow diameter of about 68 nm, and the mesoporous shell thickness of about 11 nm. The observation via SEM and TEM images of hard-template etching over time in the hollow mesoporous silica nanoparticle synthesis has shown that the suitable etching time has been determined to be 120 minutes. The synthesis time for the main reactions was shortened by more than half from 21 hours to 9 hours. Moreover, the synthesized HMSN performed as a biocompatible material with no *in vitro* toxicity at the concentration up to 250 µg/mL. This modified hard-template method with shorter synthesis time and nearly 100 nm obtained particle diameter would be meaningful for scientific research and industrial scale production.

**Acknowledgement.** This research is funded by Vietnam National Foundation for Science and Technology Development (NAFOSTED) under grant number NCUD.02-2022.17.

**CRedit authorship contribution statement.** Ngoc Hoi Nguyen: Formal analysis, Methodology, Writing-Original draft preparation, Visualization, Performing the analysis, Data curation. Cuu Khoa Nguyen: Formal analysis, Software, Conceiving and designing the analysis. Dai Hai Nguyen: Investigation, Funding acquisition, Supervision, Writing- Reviewing and Editing.

**Declaration of competing interest.** The authors declare that they have no known competing financial interests or personal relationships that could have appeared to influence the work reported in this paper.

#### REFERENCES

1. Karaman D. Ş. and H. Kettiger. - Silica-based nanoparticles as drug delivery systems: Chances and challenges, in Alexandru M. G. (Eds.), *Inorganic Frameworks as Smart Nanomedicines*, Elsevier Inc., Amsterdam, 2018, pp. 1-40. <https://doi.org/10.1016/B978-0-12-813661-4.00001-8>.
2. Yanagisawa T., T. Shimizu K. Kuroda, and Kato C. - Trimethylsilyl derivatives of alkyltrimethylammonium–kanemite complexes and their conversion to microporous SiO<sub>2</sub> materials, *Bulletin of the Chemical Society of Japan* **63** (5) (1990) 1535-1537. <https://doi.org/10.1246/bcsj.63.1535>.
3. Zhou Y., G. Quan, Q. Wu, X. Zhang, B. Niu, B. Wu, Y. Huang, X. Pan, and C. Wu. - Mesoporous silica nanoparticles for drug and gene delivery, *Acta pharmaceutica sinica B* **8** (2) (2018) 165-177. DOI: 10.1016/j.apsb.2018.01.007.
4. Narayan R., U.Y. Nayak, A.M. Raichur, and S. Garg. - Mesoporous Silica Nanoparticles: A Comprehensive Review on Synthesis and Recent Advances, *Pharmaceutics* **10** (3) (2018) 118. DOI:10.3390/pharmaceutics10030118.
5. Thi T. T. N., Tran T. V., Tran N. Q., Nguyen C. K., and Nguyen D. H. - Hierarchical self-assembly of heparin-PEG end-capped porous silica as a redox sensitive nanocarrier for doxorubicin delivery, *Materials Science and Engineering C* **70** (2017) 947-954. <https://doi.org/10.1016/j.msec.2016.04.085>.
6. Chen Y. - Synthesis of hollow mesoporous silica nanoparticles by silica-etching chemistry for biomedical applications, in Chen, Y. (Eds.), *Design, Synthesis, Multifunctionalization and Biomedical Applications of Multifunctional Mesoporous Silica-Based Drug Delivery*

- Nanosystems, Springer, Berlin, Heidelberg, 2016, pp. 31-46. [https://doi.org/10.1007/978-3-662-48622-1\\_2](https://doi.org/10.1007/978-3-662-48622-1_2).
7. Bao Y., Shi C., Wang T., Li X., and Ma J. - Recent progress in hollow silica: Template synthesis, morphologies and applications, *Microporous and Mesoporous Materials* **227** (2016) 121-136. <https://doi.org/10.1016/j.micromeso.2016.02.040>.
  8. Gonçalves M. - Sol-gel silica nanoparticles in medicine: A natural choice. Design, synthesis and products, *Molecules* **23** (8) (2018) 2021. doi: 10.3390/molecules23082021.
  9. Chen F., Hong H., Shi S., Goel S., Valdovinos H. F., Hernandez R., Theuer C. P., Barnhart T. E., and Cai W. - Engineering of hollow mesoporous silica nanoparticles for remarkably enhanced tumor active targeting efficacy, *Scientific reports* **4** (1) (2014) 1-10. doi: 10.1038/srep05080.
  10. Nguyen Thi N. T., Pham Tran L. P., Le N. T. T., Cao M. T., Tran T. N., Nguyen N. T., Nguyen C. H., Nguyen D. H., Than V. T., and Le Q. T. - The engineering of porous silica and hollow silica nanoparticles to enhance drug-loading capacity, *Processes* **7** (11) (2019) 805. <https://doi.org/10.3390/pr7110805>.
  11. Thi N. T. N. and Nguyen D. H. - Hollow mesoporous silica nanoparticles fabrication for anticancer drug delivery, *Vietnam Journal of Science and Technology* **58** (1) (2020) 39. <https://doi.org/10.15625/2525-2518/58/1/14267>.
  12. Mitchell M. J., Billingsley M. M., Haley R. M., M.E. Wechsler, N.A. Peppas, and R. Langer. - Engineering precision nanoparticles for drug delivery, *Nature Reviews Drug Discovery*. **20** (2) (2021) 101-124. <https://doi.org/10.1038/s41573-020-0090-8>.
  13. Nguyen T. N. T., N. T. T. Le, N. H. Nguyen, B. T. K. Ly, T. D. Nguyen, and D. H. Nguyen - Aminated hollow mesoporous silica nanoparticles as an enhanced loading and sustained releasing carrier for doxorubicin delivery, *Microporous and Mesoporous Materials* **309** (2020) 110543. <https://doi.org/10.1016/j.micromeso.2020.110543>.
  14. Desai M. P., V. Labhsetwar, E. Walter, R. J. Levy, and G. L. Amidon. - The mechanism of uptake of biodegradable microparticles in Caco-2 cells is size dependent, *Pharmaceutical research*. **14** (11) (1997) 1568-1573. <https://doi.org/10.1023/A:1012126301290>.
  15. Nguyen T. N. T., D. H. N. Tran, L. G. Bach, and D. H. Nguyen - Surface PEGylation of hollow mesoporous silica nanoparticles via aminated intermediate, *Progress in Natural Science: Materials International* **29** (6) (2019) 612-616. <https://doi.org/10.1016/j.pnsc.2019.10.002>.
  16. Han Y., Z. Lu, Z. Teng, J. Liang, Z. Guo, D. Wang, M. Y. Han, and W. Yang. - Unraveling the growth mechanism of silica particles in the stober method: in situ seeded growth model, *Langmuir*. **33** (23) (2017) 5879-5890. <https://doi.org/10.1021/acs.langmuir.7b01140>.
  17. Vazquez N. I., Z. Gonzalez, B. Ferrari, and Y. Castro - Synthesis of mesoporous silica nanoparticles by sol-gel as nanocontainer for future drug delivery applications, *Boletín de la Sociedad Española de Cerámica y Vidrio* **56** (3) (2017) 139-145. <https://doi.org/10.1016/j.bsecv.2017.03.002>.
  18. Masalov V., N. Sukhinina E. Kudrenko, and G. Emelchenko - Mechanism of formation and nanostructure of Stöber silica particles, *Nanotechnology* **22** (27) (2011) 275718. doi: 10.1088/0957-4484/22/27/275718.

19. Li W., Y. Tian, C. Zhao, B. Zhang, H. Zhang, Q. Zhang, and W. Geng. - Investigation of selective etching mechanism and its dependency on the particle size in preparation of hollow silica spheres, *Journal of Nanoparticle Research* **17** (12) (2015) 1-11. <https://doi.org/10.1007/s11051-015-3291-z>.
20. Sikora A., A. G. Shard, and C. Minelli. - Size and  $\zeta$ -potential measurement of silica nanoparticles in serum using tunable resistive pulse sensing, *Langmuir* **32** (9) (2016) 2216-2224. <https://doi.org/10.1021/acs.langmuir.5b04160>.
21. Danaei M., M. Dehghankhold, S. Ataei, F. Hasanzadeh Davarani, R. Javanmard, A. Dokhani, S. Khorasani, and M. Mozafari. - Impact of particle size and polydispersity index on the clinical applications of lipidic nanocarrier systems, *Pharmaceutics*. **10** (2) (2018) 57. DOI: 10.3390/pharmaceutics10020057.
22. Guston D. H. - *Encyclopedia of nanoscience and society*, SAGE Publications Inc., Washington DC, 2010.
23. Peer D., J. Kar, S. Hong, O. Farokhzad, and L. R. Margalit. - Nanocarriers as an emerging platform for cancer therapy, *Nature Nanotechnology* **2** (12) (2007) 751-60. doi:10.1038/nnano.2007.387.
24. Jiao Y., J. Guo, S. Shen, B. Chang, Y. Zhang, X. Jiang, and W. Yang. - Synthesis of discrete and dispersible hollow mesoporous silica nanoparticles with tailored shell thickness for controlled drug release, *Journal of Materials Chemistry*. **22** (34) (2012) 17636-17643. DOI:10.1039/C2JM31821K.
25. Cheng K., Y. Zhang, Y. Li, Z. Gao, F. Chen, K. Sun, P. An, C. Sun, Y. Jiang, and B. Sun. - A novel pH-responsive hollow mesoporous silica nanoparticle (HMSN) system encapsulating doxorubicin (DOX) and glucose oxidase (GOX) for potential cancer treatment, *Journal of Materials Chemistry B*. **7** (20) (2019) 3291-3302. <https://doi.org/10.1039/C8TB03198C>.
26. Khoeini M., A. Najafi, H. Rastegar, and M. Amani. - Improvement of hollow mesoporous silica nanoparticles synthesis by hard-templating method via CTAB surfactant, *Ceramics International*. **45** (10) (2019) 12700-12707. <https://doi.org/10.1016/j.ceramint.2019.03.125>.
27. Dubey R., Y. Rajesh, and M. More. - Synthesis and characterization of SiO<sub>2</sub> nanoparticles via sol-gel method for industrial applications, *Materials Today: Proceedings*. **2** (4-5) (2015) 3575-3579. DOI:10.1016/j.matpr.2015.07.098.
28. Joseph, E. and G. Singhvi. - Multifunctional nanocrystals for cancer therapy: a potential nanocarrier, in Alexandru M. G. (Eds.) *Nanomaterials for drug delivery and therapy*, Elsevier Inc., Amsterdam, 2019, pp. 91-116. <https://doi.org/10.1016/B978-0-12-816505-8.00007-2>.
29. Scarlett, N.V. and I.C. Madsen. - Effect of microabsorption on the determination of amorphous content via powder X-ray diffraction, *Powder Diffraction*. **33** (1) (2018) 26-37. DOI: <https://doi.org/10.1017/S0885715618000052>.